Desalination and Water Treatment
www.deswater.com

doi: 10.1080/19443994.2015.1022802

57 (2016) 7209–7218
April

Taylor & Francis
Taylor & Francis Group

Adsorption of Ni(II) ions from aqueous solution onto a fungus *Pleurotus ostreatus*

Tahira Mahmood, Afsar Khan, Abdul Naeem*, Muhammad Hamayun, Mairman Muska, Muhammad Farooq, Fida Hussain

National Centre of Excellence in Physical Chemistry, University of Peshawar, Peshawar 25120, Pakistan, Tel. +92 91 9218407; email: tahiramah@yahoo.com (T. Mahmood), Tel. +92 91 9216766; email: afsarkhan9343@gmail.com (A. Khan), Tel. +92 91 9218480; email: naeeem64@yahoo.com (A. Naeem), Tel. +92-91-9216766; emails: hamayunf@yahoo.com (M. Hamayun), mmuskachem@yahoo.com (M. Muska), farooq_khann@yahoo.com (M. Farooq), fida_durrani@yahoo.com (F. Hussain)

Received 17 July 2014; Accepted 28 January 2015

ABSTRACT

In this study, the sorption behavior of *Pleurotus ostreatus* toward Ni(II) is examined with respect to pH, temperature, contact time, and concentration. The good correlation coefficient and close agreement between experimental and theoretical values of biosorption capacity confirm that the pseudo-second-order kinetic model is best applicable to the kinetics data. The sorption of Ni(II) is found to be dependent upon the pH and temperature of the solution. The adsorption of Ni(II) onto *P. ostreatus* is maximum at higher pH values and decreases with an increase in temperature in the range of 298–318 K. Both X_m and K_b values decrease with increase in temperature, indicating the exothermic nature of the process. Different thermodynamic parameters were calculated for adsorption of Ni(II) onto *P. ostreatus*. The negative value of ΔS indicates a decrease in randomness at the solid/liquid interface. The values of isosteric heat of adsorption are decreasing with increases in surface coverage, which reveal the heterogeneous nature of the solid surface. The FTIR spectra show that the carbonyl groups of *P. ostreatus* are responsible for adsorption of Ni(II) onto *P. ostreatus*.

Keywords: Biosorption; Nickel; *Pleurotus ostreatus*; Langmuir isotherm; Isosteric heat

1. Introduction

Environmental pollution has become a serious threat to public health [1,2]. Nickel is a toxic heavy metal mostly present in water as Ni(II) ions. Nickel is used in a large number of metabolic processes such as hydrogen metabolism, methane biogenesis, and acetogenesis. It is also used in the hydrogenation of oils. Several industries like electroplating, mining, nickel alloys, steel manufacturing, and batteries are responsible for the release of pollutants into the water [3]. The recommended permissible limit of nickel in drinking water is 0.02 mg L^{-1} [4]. Toxicity of Ni(II) is concerned with enzyme inhibition, chest pain, vomiting, diarrhea, and dizziness [5]. It also causes skin, lung, and kidney diseases, and severe weakness in the body. Nickel is carcinogenic in nature as it affects the deoxyribonucleic acid linkages [6].

The concentration of nickel in groundwater in many areas of Pakistan varies from 0 to 3.66 mg L^{-1}

*Corresponding author.

which exceeds the recommended permissible limit in groundwater [7]. Moreover, nickel is found to exceed its permissible limit in drinking water of Hayat Abad, Akbarpura, Palosi Drain of Peshawar, Gadoon, and Hasan Abdal in Khyber Pakhtunkhwa province of Pakistan, Kalalanwala, Kalar Kahar, Kasur, and Sialkot city of Punjab, Karachi, Sehwan, Machar Lake Jamshoro of Sindh in Pakistan [8].

Several methods including reverse osmosis, electrodialysis, ultrafiltration, ion exchange, precipitation, phytoremediation, and solvent extraction are used for the removal of metal ions from water. Some of the disadvantages of these traditional methods are sludge formation, use of large amounts of chemicals, incomplete recovery of metals, addition of anti-precipitants, replacement of membranes, and energy consuming [8]. Ion-exchange adsorption is a versatile technique which is conventionally tested for the removal of toxins from water.

Biosorption is an economical process which has been used for the removal of many toxic pollutants from drinking water because of its low cost, high efficiency, easy regeneration, and minimization of chemical and biological sludge. Various biosorbents such as aliginate gel beads, chitosan, kaolinite, *Boletus edulis*, and *Russula delica* have been used for the recovery of heavy metal ions from water [9].

Mushroom family is found to be the best biosorbents for decontamination of water. Macro fungus can be grown in natural habitat and is easily available in many places of the world [10]. It is highly stable in both the acidic and basic medium. *Pleurotus ostreatus* is an edible mushroom grown on trees and woods in nature. The inedible part of *P. ostreatus* has been chosen for the metal adsorption because of its easy availability, fast kinetics, and high adsorption capacity [11,12].

2. Materials and methods

2.1. Reagents

All chemicals used in the current experiments were of analytical grade. Initially, 1,000 mg L^{-1} stock solution was prepared from $NiCl_2$ (Scharlau) in a volumetric flask. All glasswares were washed with distilled water and 10% HNO_3, respectively, and at the end were rinsed with deionized water. The working solutions of desired concentrations ranging from 5 to 250 mg L^{-1} were prepared from 1,000 mg L^{-1} stock solution of nickel. The initial pH of the solution was adjusted using 0.1 M HCl/NaOH solutions.

2.2. Preparation of biosorbent

The fungus *P. ostreatus*, also called mushroom, was purchased from local markets in Peshawar city, Pakistan. It was initially washed with water and then with deionized water to remove the dust particles and water-soluble impurities. The materials were placed in open sunlight for two days and then dried in oven at 80°C. The dried materials were powdered and passed through 200 mm mesh. The powdered sample was characterized and was then effectively used for the Ni(II) adsorption from aqueous solution.

2.3. Characterization

P. ostreatus was characterized by scanning electron microscopy (SEM) model JSM 5910 JEOL. The elemental analysis of the sample was carried out by energy dispersive X-ray (EDX) model INCA 200. The surface area was determined using the surface area analyzer model Quanta Chrome Nova 2200e. Before analysis, the sample was degassed at 100°C for 1 h. The Brunauer–Emmett–Teller model was tested to assess the surface area of *P. ostreatus*. The powder sample of *P. ostreatus* was subjected to X-ray diffrectometry (XRD) analysis using the XRD model JDX-3532. Thermal analyses of the *P. ostreatus* were performed in thermogravimetric analyzer model Perkin-Elmer 6300. Weighted sample was subjected under controlled heating and the heating rate was 10°C min^{-1}. The sample was heated in the temperature range of 30–1,000°C. The change in weight was calculated from the difference in weight of the *P. ostreatus* before and after heating. Fourier transform infrared spectroscopy (FTIR) model Shimadzu 8201 PC was used for IR analysis of *P. ostreatus*. The point of zero charge (PZC) of *P. ostreatus* was determined by salt addition method.

2.4. Sorption studies

Batch adsorption experiments were conducted in 100 mL conical flask with 0.1 g biosorbent and 40 mL of Ni(II) solutions. The pH of the system was adjusted in the range of 2–8. The reaction flasks were equilibrated in a Wise Bath shaker at 120 rpm for 24 h at 298 K. Suspensions were then filtered and the filtrates were analyzed by Perkin-Elmer Analyst 800 atomic absorption spectrometer. The amount of Ni(II) adsorbed was determined from the difference between initial and final concentration. The temperature studies were conducted at pH 6 and at 308, 318, and 328 K. The solid residue before and after Ni(II) adsorption was characterized by FTIR spectroscopy.

3. Results and discussion

3.1. Characterization

3.1.1. Scanning electron microscopy/energy dispersive X-ray

The scanning electron micrographs recorded for *P. ostreatus* at magnifications of 3,000× and 2,000× are given in Fig. 1. The SEM images indicate that the *P. ostreatus* is irregular in shape while its EDX spectrum (Fig. 2) shows that carbon and oxygen are the major elements in addition to K. The weight percent of C, O, and K are recorded to be 51.7, 46.3, and 2.26%, respectively, which are almost comparable with findings reported by Tay et al. [13].

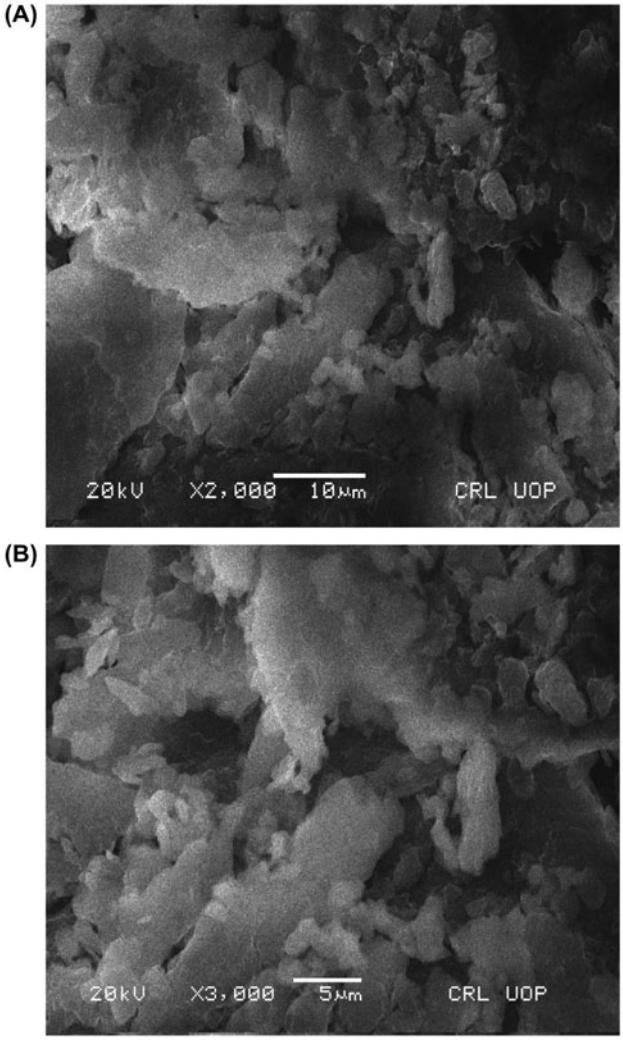

Fig. 1. SEM images of *P. ostreatus* at (A) 2,000× (B) at 3,000×.

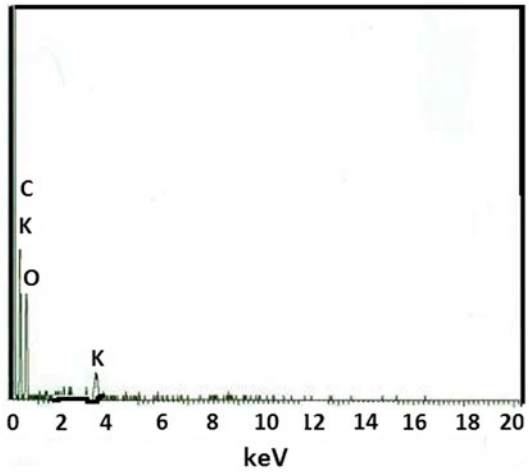

Fig. 2. EDX spectrum of *P. ostreatus*.

3.1.2. Surface area

The surface area of *P. ostreatus* is found to be 81 $m^2 g^{-1}$, which is greater than the surface area (3.7 $m^2 g^{-1}$) reported by Islek et al. [14] for the same species and is comparable to the one reported by Swayampakula et al. [15] for chitosan-coated perlite beads.

3.1.3. X-ray diffrectometry

The XRD spectrum of *P. ostreatus* indicated the *P. ostreatus* to be amorphous in nature which is in agreement with the spectra of *Moringa oleifera* bark [16].

3.1.4. Thermogravemetric analysis and derivative thermogravimetry

The Thermogravemetric analysis (TGA)/derivative thermogravimetry (DTG) analyses of biomass were carried out in the temperature range of 30–1,000˚C. The total weight loss was recorded to be 93%, which was observed in three stages (Fig. 3). The first weight loss (18%) occurred in the temperature range of 50–250˚C, which is assigned to the dehydration of the biomass. The second weight loss (43%) up to 390˚C is due to the conversion of organic matter to atmospheric gases i.e. CO_2 and CO [17]. The third weight loss (31%) up to 900˚C may be due to the passive pyrolysis. The TGA results were strongly supported by the DTG curve. Similar TGA/DTG results were reported by Yang et al. [18] while studying the thermal behavior of different fungi.

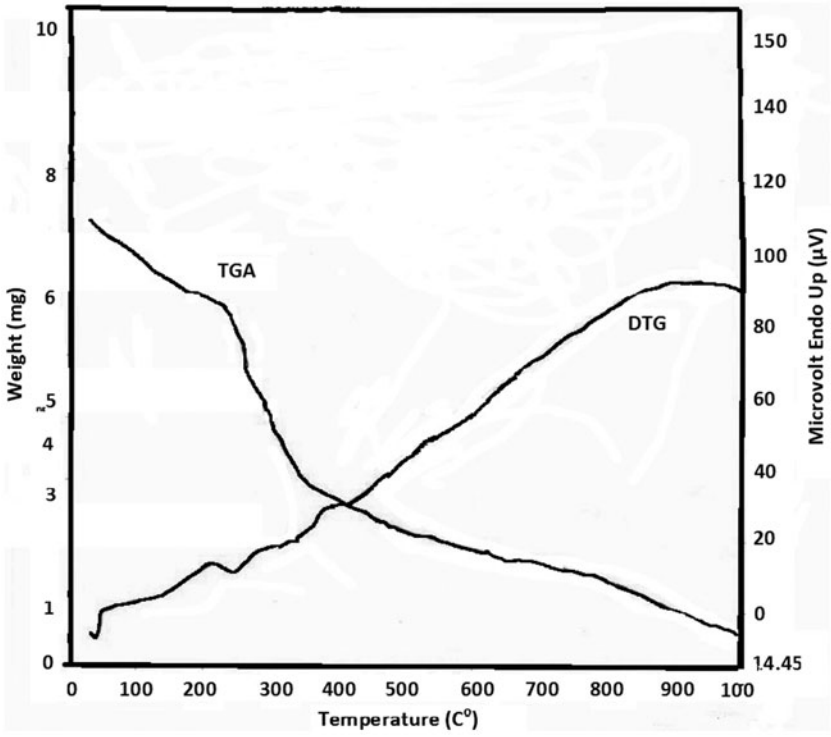

Fig. 3. TGA and DTG of *P. ostreatus*.

3.1.5. Fourier transform infrared spectroscopy

FTIR spectrum of *P. ostreatus* has been shown in Fig. 4(A). The broad absorption band in the range of 3,500–3,000 cm^{-1} generally indicates the OH group of carbohydrate (glucose) and NH_2 group of proteins [12]. The absorption band at 2,900 cm^{-1} shows the –CH stretching vibration. The weak absorption band at 1,600 cm^{-1} indicates the C=O group of proteins. Another band at 1,050 cm^{-1} is assignable to C–O–C stretching vibration.

3.1.6. Point of zero charge

A well-known method [19] was used to determine the PZC. The data shown in Fig. 5 exhibits the PZC at pH 6.5 which is close to the value (6.1) reported by Fernandez et al. [20].

3.2. Adsorption kinetics studies

3.2.1. Effect of contact time

Kinetic study of Ni(II) adsorption onto *P. ostreatus* is carried out at different time intervals at 298 K. The

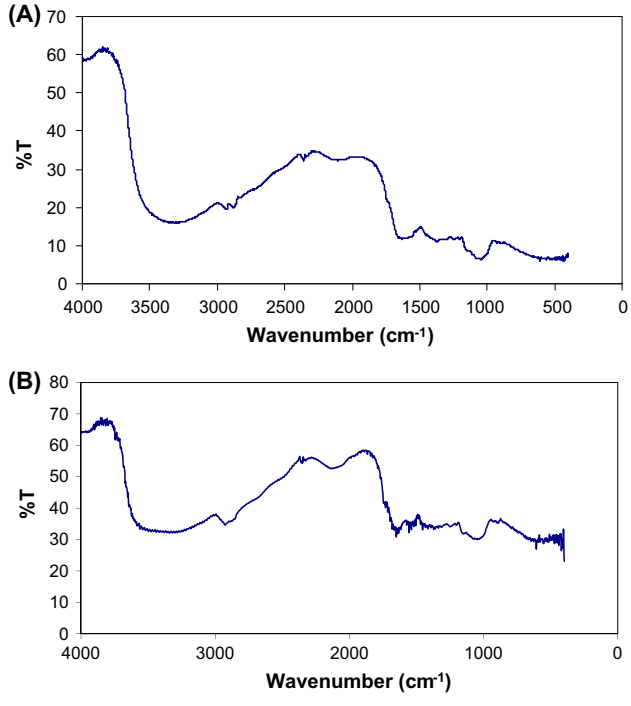

Fig. 4. FTIR spectra of *P. ostreatus* (A) before (B) after sorption of Ni(II).

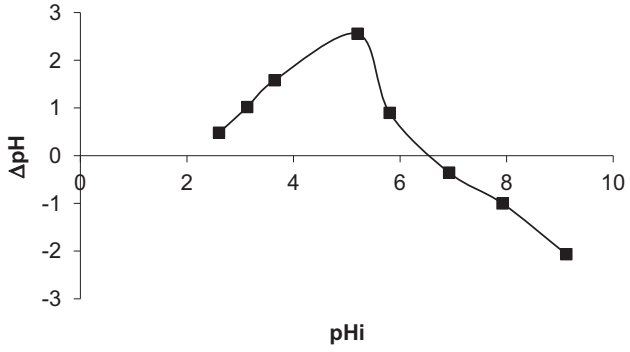

Fig. 5. PZC of *P. ostreatus* at 298 K.

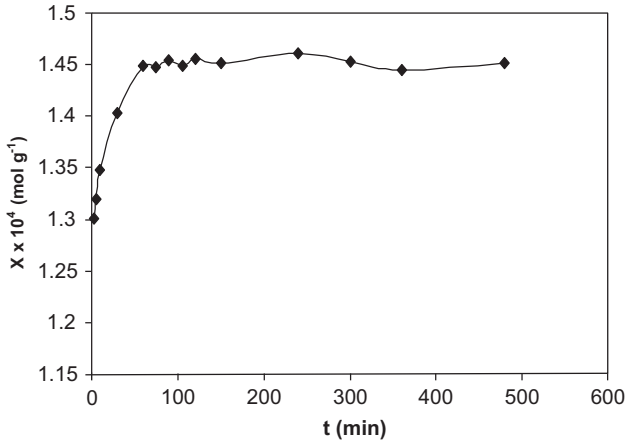

Fig. 6. Kinetic study of Ni(II) sorption by *P. ostreatus* at 298 K and pH 7.

amount of Ni(II) ions adsorbed (mol g^{-1}) is plotted vs. time (Fig. 6). It is obvious from Fig. 6 that more than 90% adsorption occurs in the first 5 min. The adsorption of Ni(II) ions increases with time and equilibrium is established in 60 min. The maximum adsorption takes place initially on the bare surface and then decreases with an increase in time as most of the available active sites are occupied by the metal ions with lapse of time. Wierzba and Latala [21] observed similar results while studying the biosorption of Ni(II) ions by *Pseudomonas fluorescens* and *Bacillus pumilus*.

3.3. Kinetic modeling

Kinetic data of Ni(II) sorption onto *P. ostreatus* was subjected to pseudo-second-order kinetic model to probe into the adsorption kinetics mechanism.

3.3.1. Pseudo-second-order kinetic model

The pseudo-second-order kinetic model may be written in the form

$$\frac{t}{q_t} = \frac{1}{k_2 q_e^2} + \frac{t}{q_e} \quad (1)$$

where q_e and q_t (mol L^{-1}) is the amount adsorbed at equilibrium and time (t), respectively, k_2 (g min^{-1} mol^{-1}) is the second-order rate constant. Plot of $\frac{t}{q_t}$ vs. t (Fig. 7) gives straight line with R^2 value >0.999. The value of q_e obtained from slope of the plot is in a close agreement with experimental value which also confirms that pseudo-second-order kinetic model is best applicable to the present kinetic data. The applicability of pseudo-second-order kinetic model is also an evidence of the chemisorption process. Reddy et al. [16] have reported almost similar results for the sorption of Ni(II) by *M. oleifera*.

3.4. Adsorption studies of Ni(II) by P. ostreatus

3.4.1. Effect of pH

In the present work, the biosorption of Ni(II) is studied in the pH range from 3 to 8 at 298 K. The adsorption of Ni(II) ions by *P. ostreatus* is minimum in the acidic pH range and increases with the increase in the pH of the medium (Fig. 8). Below PZC (6.5), the surface is positively charged due to protonation of various surface groups (i.e. carboxylic, amine, and alcoholic) whereas the surface is negatively charged above its PZC value. Above PZC, the columbic force of attraction between metal cations and the negative surface increases the adsorption of Ni(II) ions onto

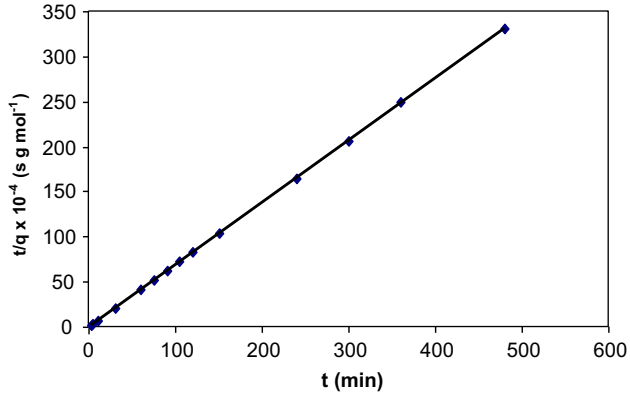

Fig. 7. Pseudo-second-order plot for Ni(II) sorption by *P. ostreatus* at pH 7 and at 298 K.

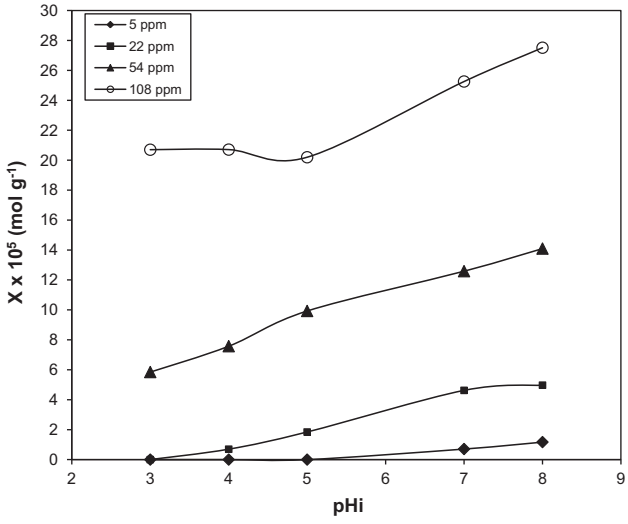

Fig. 8. Effect of pH on Ni(II) sorption by *P. ostreatus* at 298 K.

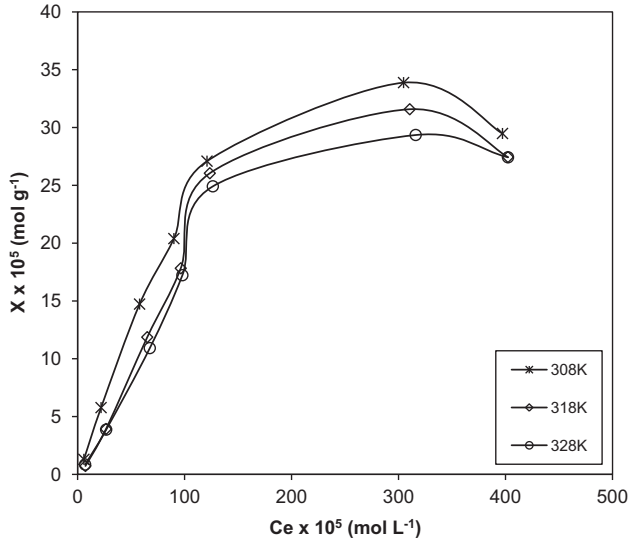

Fig. 9. Effect of temperature on Ni(II) sorption by *P. ostreatus* at different temperatures and at pH 6.

P. ostreatus whereas below its PZC value, the repulsive forces between positive surface and metal cations prevent adsorption of Ni(II) ions onto the surface of *P. ostreatus*. Moreover, the minimum adsorption at low pH value may also be due to the competition of protons with Ni(II) ions for the same surface sites. Zhao et al. [22] reported almost similar results for sorption of Ni(II) ions from aqueous solution by dialdehyde o-phenylenediamine starch.

Moreover, the final pH of the system was noted to decrease after adsorption of Ni(II) ions by the surface of *P. ostreatus*. This decrease in equilibrium pH is pointing toward the replacement of protons from the solid surface. As such, the surface of the *P. ostreatus* becomes negatively charged, which is then neutralized by the Ni(II) ions present in the aqueous phase. It is therefore suggested that the Ni(II) adsorption takes place through a cation exchange process.

3.4.2. Effect of temperature

The effect of temperature on adsorption of Ni(II) onto *P. ostreatus* is investigated in the temperature range of 308, 318, and 328 K. Fig. 9 shows a significant effect of temperature on the adsorption of Ni(II) ions onto *P. ostreatus*. The adsorption of Ni(II) onto *P. ostreatus* decreases with the increase in temperature, which confirms an exothermic nature of the process (Fig. 9). This decrease in adsorption of Ni(II) ions onto *P. ostreatus* may be attributed to changes in the cell wall configuration of the *P. ostreatus* at high temperature. Moreover, an increase in temperature may also result in the weakening of binding forces between surface of *P. ostreatus* and metal ions and the tendency of metal ions to escape from the surface into the bulk of the solution increases. Similar results were reported for the adsorption of Ni(II) by immobilized cells of bacillus species [23].

3.5. Adsorption isotherm

3.5.1. Langmuir model

A well known Langmuir model is applied to the experimental data which describes that all the sites are energetically equivalent and rules out the interaction among the adsorbed Ni(II) ions. The linear form of this model may be written as:

$$\frac{C_e}{X} = \frac{1}{KX_m} + \frac{C_e}{X_m} \quad (2)$$

where C_e (mol L^{-1}) is the equilibrium concentration of Ni(II) ions, X (mol g^{-1}) is the adsorbed amount of Ni(II), and X_m (mol g^{-1}) stands for monolayer adsorption capacity, K_b (L g^{-1}) is the binding energy constant. The values of X_m and K_b were calculated from the slopes and intercepts of the plots between C_e/X vs. C_e (Fig. 10). Both the X_m and K_b values (Table 1) decrease with increase in temperature, which indicate an exothermic nature of the process [24]. The present values of the adsorption maxima are several times greater than many of the adsorbent reported previously [25–28], which further confirm

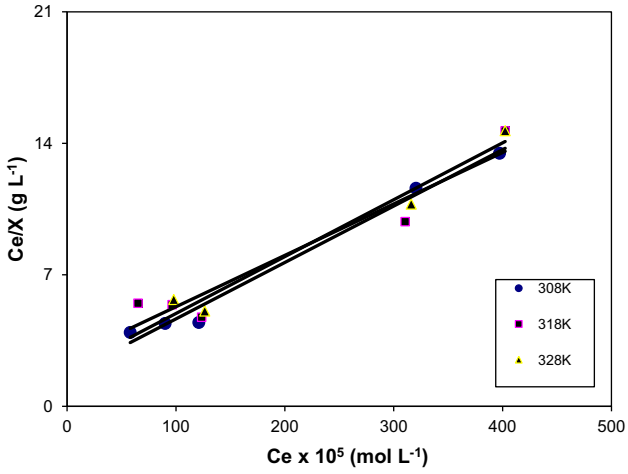

Fig. 10. Langmuir plots for Ni(II) sorption by *P. ostreatus* at different temperatures and at pH 6.

that *P. ostreatus* is an efficient biosorbent for the removal of Ni(II) from aqueous solution (Table 2).

3.6. Thermodynamic parameters

The changes in enthalpy (ΔH), entropy (ΔS) and Gibbs free energy (ΔG) for Ni(II) adsorption onto *P. ostreatus* were calculated according to the following equations:

$$\ln K_b = \frac{\Delta S}{R} - \frac{\Delta H}{RT} \quad (3)$$

$$\Delta G = \Delta H - T\Delta S \quad (4)$$

where K_b is the Langmuir parameter. The enthalpy and entropy changes were calculated from the slope and intercept by plotting of $\ln K_b$ vs. $1/T$ (Fig. 11), respectively.

The values of thermodynamic parameters for the adsorption of Ni(II) ions onto *P. ostreatus* are given in Table 3. The negative values of ΔG show the spontaneous nature of the process and further suggest that the sorption forces are strong enough to break the barrier for Ni(II) adsorption onto *P. ostreatus*. Moreover, the decrease in negative ΔG values with increase in temperature shows that the uptake of Ni(II) by *P. ostreatus* is favored at lower temperature which is strongly supported by the negative ΔH value. Basha et al. [29] reported similar results for Ni(II) adsorption by Variegata. Moreover, Ho and Ofomaja [24] also reported negative ΔH value while studying the biosorption of cadmium by coconut copra. The negative value of ΔS in this study indicates a decrease in the randomness at solid–liquid interface after adsorption of Ni(II) onto *P. ostreatus*. The present value is closer to the ΔS value (-13 J K^{-1} mol^{-1}) reported by Adeogun et al. [30] for Mn (II) adsorption by corncob biomass.

3.7. Isosteric heat of adsorption

Adsorption experiments were conducted at different temperatures to assess the isosteric heat of adsorption ($\overline{\Delta H}$) using the following Clausius–Clapeyron equation.

$$\ln[C_e]_\theta = \frac{\Delta H}{RT} + K \quad (5)$$

Table 1
Langmuir parameters (X_m and K_b) for Ni(II) biosorption by *P. ostreatus* at different temperatures and at pH 6

Temp (K)	Slope	Intercept	K_b (L g^{-1})	$X_m \times 10^4$ (mol g^{-1})
308	2,932.9	1.65	1,774	3.4
318	2,971.7	2.56	1,158	3.3
328	2,841	3.04	932	3.5

Table 2
Comparative adsorption capacity of different biosorbents for the uptake of Ni(II) ions

Biosorbent	X_m (mg g^{-1})	References
Irish peat moss	14.5	[25]
Lignin	5.98	[26]
Chitosan immobilized with reactive blue 2 dye	8.5	[27]
Mucor rouxii	6.34	[28]
P. ostreatus	20.71	Present work

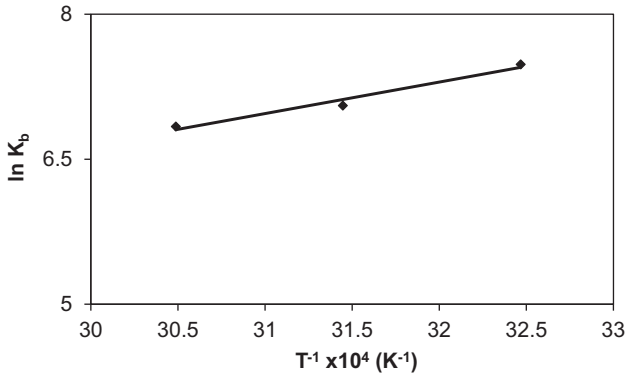

Fig. 11. Plot of ln K_b vs. T^{-1} for sorption of Ni(II) by *P. ostreatus* at pH 6.

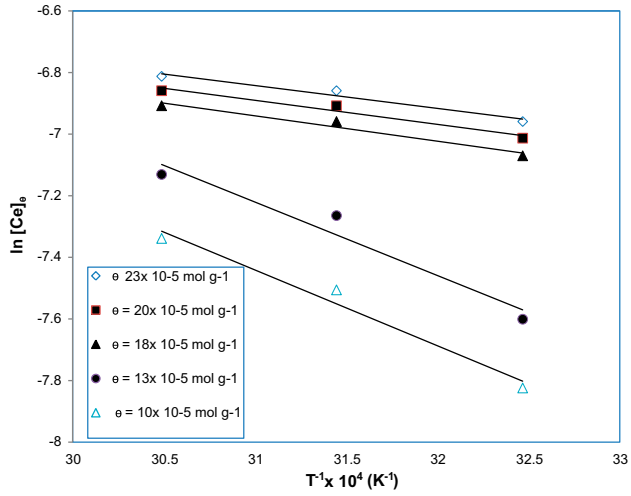

Fig. 12. Plot of $\ln[C_e]_\theta$ vs. T^{-1} for Ni(II) sorption by *P. Osreatus* at pH 6.

Table 3
Thermodynamic parameters for the sorption of Ni(II) by *P. ostreatus* at different temperatures and at pH 6

Temp (K)	ΔH (kJ mol^{-1})	ΔS (J K^{-1} mol^{-1})	ΔG (kJ mol^{-1})
308			−19.08
318	−30.47	−36.96	−18.71
328			−18.34

where C_e (mol L^{-1}) represents the equilibrium concentration of Ni(II) ions in the solution, θ represents the surface coverage, and R is the gas constant (8.314 J mol^{-1} K^{-1}). The values of isosteric heat of adsorption ($\overline{\Delta H}$) were measured from the slopes of the plots of $[\ln C_e]_\theta$ vs. $1/T$ (Fig. 12). The negative values of $\overline{\Delta H}$ (Table 4) show that the uptake of Ni(II) by *P. ostreatus* decreases with the increase in temperature, which is similar to the conclusions drawn from the enthalpy (ΔH) and Gibbs free energy (ΔG) of adsorption. Fig. 13 shows that the magnitude of $\overline{\Delta H}$ decreases with increasing the surface loading [θ]. The variation in the values of $\overline{\Delta H}$ with surface coverage (Fig. 13) indicates that the *P. ostreatus* is energetically heterogeneous. Similar results were also reported by Mustafa et al. [31] while studying temperature effect on phosphate sorption by MnO_2.

3.8. FTIR studies

The solid residue of *P. ostreatus* before and after adsorption was characterized by FTIR (Fig. 4). A new absorption band at around 1,600–1,650 cm^{-1} appears after adsorption, which is assigned to the binding of Ni(II) ions onto carbonyl (C=O) groups available on the surface. Similar vibration bands were reported by Xiangliang et al. [12] for Pb (II) adsorption by *P. ostreatus*. Moreover, similar changes in the IR spectra were also observed for Ni(II) adsorption by thermally decomposed leaf [32].

Table 4
Isosteric heat of Ni(II) sorption on *P. ostreatus* at pH 6

$X \times 10^4$ (mol g^{-1})	$\overline{\Delta H}$ (kJ mol^{-1})	R^2
2.3	−6.17	0.96
2	−6.49	0.96
1.8	−6.84	0.96
1.3	−19.82	0.94
1	−20.44	0.97

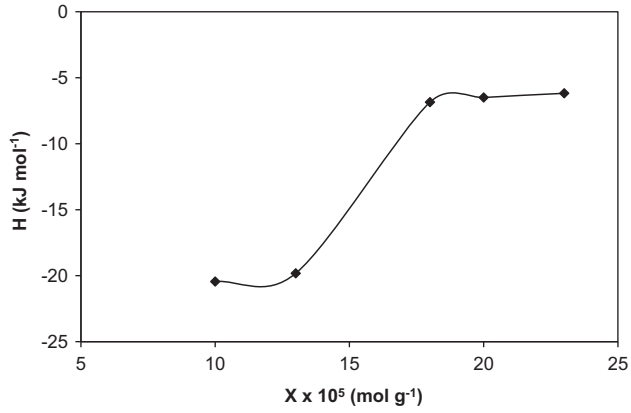

Fig. 13. Isosteric heat ($\overline{\Delta H}$) of Ni(II) sorption by *P. ostreatus* as a function of surface coverage [θ].

4. Conclusion

Biosorption of Ni(II) by *P. ostreatus* was observed to increase with the increase in pH, while a decrease in Ni(II) uptake was observed with increase in temperature. The values of X_m and K_b were found to decrease with the rise in temperature, which confirmed the exothermic nature of the process. The values of all the thermodynamic parameters (ΔG, ΔH, and ΔS) were found to be negative, which points toward spontaneous, exothermic, and a decrease randomness at the solid–liquid interface. The dependency of isosteric heat ($\overline{\Delta H}$) of adsorption on the surface coverage (θ) also indicates the heterogeneous nature of the *P. ostreatus* surface.

References

[1] T. Mahmood, S.U. Din, A. Naeem, S. Tasleem, A. Alum, S. Mustafa, Kinetics, equilibrium and thermodynamics studies of arsenate adsorption from aqueous solutions onto iron hydroxide, J. Ind. Eng. Chem. 20 (2014) 3234–3242.

[2] M. Hamayun, T. Mahmood, A. Naeem, M. Muska, S.U. Din, M. Waseem, Equilibrium and kinetics studies of arsenate adsorption by $FePO_4$, Chemosphere 99 (2014) 207–215.

[3] T.G. Muhammad, T.G. Chuah, Y. Robiah, A.R Suraya, T.S.Y. Choong, Single and binary adsorptions isotherms of Cd(II) and Zn(II) on palm kernel shell based activated carbon, Desalin. Water Treat. 29 (2011) 140–148.

[4] M. Yang, Y. Zhao, X. Sun, X. Shao, D. Li, Adsorption of Sn(II) on expanded graphite: Kinetic and equilibrium isotherm studies, Desalin. Water Treat. 52 (2014) 283–292.

[5] L. Zhirong, Y. Rong, S. Xinhuai, Adsorption of Th(IV) by peat moss, Desalin. Water Treat. 28 (2011) 196–201.

[6] A. Suazo-Madrid, L. Morales-Barrera, E. Aranda-García, E. Cristiani-Urbina, Nickel(II) biosorption by *Rhodotorula glutinis*, J. Ind. Microbiol. Biotechnol. 38 (2011) 51–64.

[7] M.U. Haq, R.A. Khattak, H.K. Puno, M.S. Saif, K.S. Memon, Surface and ground water contamination in NWFP and Sindh provinces with respect to trace elements, Int. J. Agri. Biol. 7 (2005) 214–217.

[8] S. Kelesoglu, Comparative adsorption studies of heavy ions on chitin and chitosan biopolymers, Thesis Master of Science in Chemistry, Institute of Technology, Izmir, Turkey, 2007.

[9] J.C. Moreno-Piraján, V.S. Garcia-Cuello, L. Giraldo, The removal and kinetics study of Mn, Fe, Ni and Cu ions from wastewater onto activated carbon from coconut shells, Adsorption 17 (2011) 505–514.

[10] N. Das, Metals biosorption by using mushrooms, Nat. Prod. Radi. 4 (2005) 454–457.

[11] A. Naeem, A. Khan, T. Mahmood, M. Hamayun, M. Waseem, Kinetics, equilibrium and thermodynamic studies of Mn(II) biosorption from aqueous solution onto *Pleurotus ostreatus*, J. Chem. Soc. Pak. 36 (2014) 788–797.

[12] P. Xiangliang, W. Jianlong, Z. Daoyong, Biosorption of Pb(II) by *Pleurotus ostreatus* immobilized in calcium alginate gel, Process Biochem. 40 (2005) 2799–2803.

[13] C.C. Tay, H.H. Liew, C. Yin, S. Abdul-Talib, S. Surif, A.A. Suhaimi, S.K. Yong, Biosorption of cadmium ions using *Pleurotus ostreatus* growth kinetics, isotherm study and biosorption mechanism, Chem. Eng. J. 28 (2011) 825–830.

[14] C. Islek, A. Sinag, I. Akata, Investigation of biosorption behavior of methylene blue on *Pleurotus ostreatus* (Jacq.) P. Kumm, Clean, 36 (2008) 387 –692.

[15] K. Swayampakula, V.M. Boddu, S.K. Nadavala, K. Abburi, Competitive adsorption of Cu (II), Co (II) and Ni(II) from their binary and tertiary aqueous solutions using chitosan-coated perlite beads as biosorbent, J. Hazard. Mater. 170 (2009) 680–689.

[16] D.H.K. Reddy, D.K.V. Ramana, K. Seshaiah, A.V.R. Reddy, Biosorption of Ni(II) from aqueous phase by *Moringa oleifera* bark, a low cost biosorbent, Desalination 268 (2011) 150–157.

[17] L. Odochian, C. Moldoveanu, A.M. Mucanu, G. Carja, Contributions to the thermal degradation mechanism under nitrogen atmosphere of PTFE by TG FTIR analysis. Influence of additive nature, Thermochim. Acta 526 (2011) 22–28.

[18] X. Yang, Y. Zeng, F. Ma, X. Zhang, H. Yu, Effect of biopretreatment on thermogravimetric and chemical characteristics of corn stover by different white rot fungi, Bioresour. Technol. 101 (2010) 5475–5479.

[19] T. Mahmood, S.U. Din, A. Naeem, S. Mustafa, M. Waseem, M. Hamayun, Adsorption of arsenate from aqueous solution on binary mixed oxide of iron and silicon, Chem. Eng. J. 192 (2012) 90–98.

[20] M.E. Fernandez, G.V. Nunell, P.R. Bonelli, A.L. Cukierman, Effectiveness of *Cupressus sempervirens* cones as biosorbent for the removal of basic dyes from aqueous solutions in batch and dynamic modes, Bioresour. Technol. 101 (2010) 9500–9507.

[21] S. Wierzba, A. Latala, Biosorption lead (II) and nickel (II) from an aqueous solution by bacterial biomass, Pol. J. Chem. Tech. 12 (2010) 72–78.

[22] P. Zhao, J. Jiang, F. Zhang, W. Zhao, J. Liu, R. Li, Adsorption separation of Ni(II) ions by dialdehyde o-phenylenediamine starch from aqueous solution, Carbohydr. Polym. 81 (2010) 751–757.

[23] A. Tahir, R. Shehzadi, B. Mateen, S. Univerdi, O. Karacoban, Biosorption of nickel (II) from effluent of electroplating industry by immobilized cells of Bacillus species, Eng. Life Sci. 9 (2009) 462–467.

[24] Y. Ho, A.E. Ofomaja, Biosorption thermodynamics of cadmium on coconut copra meal as biosorbent, Biochem. Eng. J. 30 (2006) 117–123.

[25] B. Sen Gupta, M. Curran, S. Hasan, T.K. Ghosh, Adsorption characteristics of Cu and Ni on Irish peat moss, J. Environ. Manage. 90 (2009) 954–960.

[26] X. Guo, S. Zhang, X.Q. Shan, Adsorption of metal ions on lignin, J. Hazard. Mater. 151 (2008) 134–142.

[27] H.L. Vasconcelos, V.T. Fávere, N.S. Gonçalves, M.C.M. Laranjeira, Chitosan modified with reactive blue 2 dye on adsorption equilibrium of Cu(II) and Ni(II) ions, React. Funct. Polym. 67 (2007) 1052–1060.

[28] G. Yan, T. Viraraghavan, Heavy-metal removal from aqueous solution by fungus *Mucor rouxii*, Water Res. 37 (2003) 4486–4496.

[29] S. Basha, S. Jaiswar, B. Jha, On the biosorption, by brown seaweed, *Lobophora variegata*, of Ni(II) from aqueous solutions: Equilibrium and thermodynamic studies, Biodegradation 21 (2010) 661–680.
[30] A.I. Adeogun, A.E. Ofudje, M. Kareem, O. Sarafadeen, Equilibrium, kinetic, and thermodynamic studies of the biosorption of Mn(II) ions from aqueous solution by raw and acid-treated corncob biomass, Bioresources 6 (2011) 4117–4134.
[31] S. Mustafa, M.I. Zaman, S. Khan, Temperature effect on the mechanism of phosphate anions sorption by β-MnO_2, Chem. Eng. J. 141 (2008) 51–57.
[32] Z. Li, S. Imaizumi, T. Katsumi, T. Inui, X. Tang, Q. Tang, Manganese removal from aqueous solution using a thermally decomposed leaf, J. Hazard. Mater. 177 (2010) 501–507.